Measurement of $D^{*\pm}$ Meson Production and Determination of $F_2^{c\bar{c}}$ at low Q^2 in Deep-Inelastic Scattering at HERA

Eva Hennekemper on behalf of the H1 Collaboration

Kirchhoff-Institut für Physik, Universität Heidelberg, Germany

DOI: `http://dx.doi.org/10.3204/DESY-PROC-2012-02/191`

Inclusive production of D* mesons in deep-inelastic *ep* scattering at HERA is studied in the range $5 < Q^2 < 100$ GeV^2 of the photon virtuality and $0.02 < y < 0.7$ of the inelasticity of the scattering process. The observed phase space for the D* meson is $p_T(D*) > 1.25$ GeV and $|\eta(D*)| < 1.8$. The data sample corresponds to an integrated luminosity of 348 pb^{-1} collected with the H1 detector. Single and double differential cross sections are measured and the charm contribution $F_2^{c\bar{c}}$ to the proton structure function F_2 is determined. The results are compared to perturbative QCD predictions at next-to-leading order implementing different schemes for the charm mass treatment and with Monte Carlo models based on leading order matrix elements with parton showers.

1 Introduction

A measurement of charm production in deep-inelastic scattering at HERA based on the reconstruction of a D^* meson [1] is presented. At HERA protons of 920 GeV have been collided with electrons of 27.6 GeV. D^* meson production at HERA happens predominantly in the following way: a charm-anticharm quark pair is produced in boson gluon fusion via the interaction of a photon from the electron and a gluon from the proton. The charm quark fragments then further into a D^* meson and hadrons. The events containing D^* mesons have been measured with the H1 detector. The kinematic range in the photon virtuality Q^2 is $5 < Q^2 < 100$ GeV^2, and in the inelasticity $0.02 < y < 0.7$. In comparison to earlier H1 analysis [2] the range in transverse momentum and pseudorapidity of the D^* is extended to $p_T(D*) > 1.25$ GeV and $|\eta(D*)| > 1.8$, such that the phase space is now about a factor of two larger. The D^* meson decays in the so-called golden decay channel $D^{*\pm} \to D^0\pi_s^\pm \to K^\mp\pi^\pm\pi_s^\pm$. The three final state

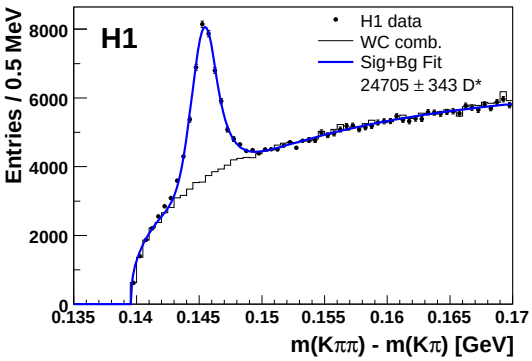

Figure 1: The mass difference of the reconstructed D^* and D^0 mesons. Data points are presented as black dots, the fit result as solid line.

particles are charged so that their tracks can be reconstructed in the central jet chambers. The D^* mesons are reconstructed with the mass difference method, where ΔM is the mass difference of the reconstructed D^* and D^0. The analysis sample comprises the full HERAII statistics and the total integrated luminosity amounts to 348 pb^{-1}. The D^* signal is shown in figure 1. In total 24705 D^* have been found, which means an increase of statistics by a factor 10 in comparison to the earlier H1 analysis [2]. In this analysis the cross sections have been determined on Born-level, the radiative effects have been corrected with using the HERACLES [3] interface. Detector effects like migrations and efficiencies have been corrected with regularized matrix unfolding. The total systematic uncertainty amounts to 7.6%, where the largest part results from the track finding efficiency with 4.1%.

1.1 QCD calculations

In this analysis the Monte Carlo (MC) generators RAPGAP [4] and CASCADE [5] have been used, which are leading order (LO) α_s QCD calculations with additional parton showers [6]. Both MCs are calculated in the fixed flavor number scheme (FFNS). The main difference of these MC generators is, that RAPGAP uses the collinear factorization with DGLAP evolution equations, while CASCADE has implemented k_T-factorization with CCFM evolution equations. In addition next-to-leading order (NLO) QCD calculations have been used in this measurement: First from HVQDIS [7], which is a FFNS calculation with collinear factorization and DGLAP evolution equations. And secondly a zero-mass variable flavor number scheme (ZM-VFNS) calculation [8] with collinear factorization and DGLAP evolution equations. In this calculation the charm quark is treated above the charm-threshold as massless parton of the proton.

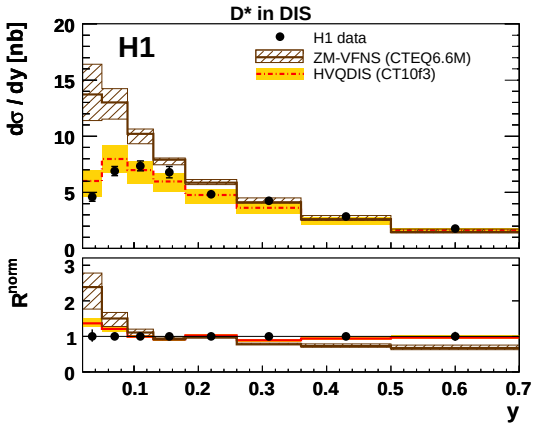

Figure 2: Single differential cross section in the inelasticity y. The H1 measurement is shown with black points with error bars denoting the systematic and statistical uncertainty of the analysis. In addition the predictions of the HVQDIS and the ZM-VFNS calculations are presented.

2 Results

The LO and NLO calculations in the FFNS give a good description of the measured D^* meson cross sections as a function of the kinematic variables of the D^* meson and of the event kinematics. The ZM-VFNS calculation fails to describe the data. In figure 2 the single differential cross section in y is presented in comparison to HVQDIS and the ZM-VFNS calculation. The uncertainty band of HVQDIS comes from the variation of the renormalization- and factorization scale, the charm mass and the fragmentation parameters, whereas the uncertainty band of the ZM-VFNS calculation includes only the scale uncertainties.

The charm cross section and $F_2^{c\bar{c}}$ are connected by the formula

$$\frac{\mathrm{d}^2\sigma^{c\bar{c}}}{\mathrm{d}x\,\mathrm{d}Q^2} = \frac{2\pi\alpha_{em}^2}{Q^4 x}\left(\left[1+(1-y)^2\right]F_2^{c\bar{c}}(x,Q^2) - y^2 F_L^{c\bar{c}}(x,Q^2)\right) \quad . \tag{1}$$

The H1 measurement comprises 50% of the total charm production phase space. The extrapolation to the full phase space was performed with

$$F_2^{c\bar{c}\,\mathrm{exp}}(\langle x\rangle,\langle Q^2\rangle) = \frac{\sigma_{\mathrm{vis}}^{\mathrm{exp}}(y,Q^2)}{\sigma_{\mathrm{vis}}^{\mathrm{theo}}(y,Q^2)} \cdot F_2^{c\bar{c}\,\mathrm{theo}}(\langle x\rangle,\langle Q^2\rangle) \quad , \tag{2}$$

where $\sigma_{vis}^{theo}(y,Q^2)$ and $F_2^{c\bar{c}theo}(x,Q^2)$ are taken from the HVQDIS prediction. This extrapolation introduces two additional uncertainties to the measurement. To determine the 'extrapolation-' uncertainty the theory parameters within HVQDIS have been varied and the 'model-' uncertainty was estimated by performing the extrapolation procedure with another model, here from CASCADE. Figure 3 (left) displays the extracted $F_2^{c\bar{c}}$. An independent H1 measurement [9]

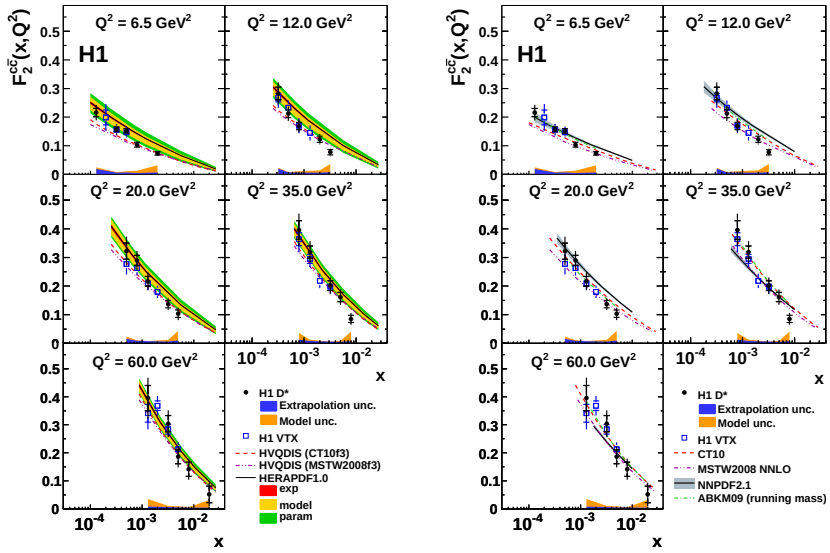

Figure 3: The extracted $F_2^{c\bar{c}}$ (black points), compared to H1 lifetime measurement (blue squares), HVQDIS and HERAPDF1.0 (on the left) and to global fit PDFs (on the right).

using lifetime information is shown too. These two H1 measurements are in good agreement. In addition the data is compared to HVQDIS predictions with two different parton density functions (PDFs) and to the HERAPDF1.0 expectation [10] in this figure. Both predictions fit well the measurement. This implies that the gluon PDF found in scaling violations of inclusive DIS cross section measurements agrees well with the gluon density from the D^* measurement. In figure 3 (right) the data is further compared to different PDFs from global fits of CT10 [11], MSTW2008 NNLO [12], NNPDF2.1 [13] in the general mass variable flavor number scheme (GMVFNS) and of ABKM09 [14] in the FFNS. The experimental uncertainty of the analysis are of the same size as the spread of the predictions. Overall, these predictions show good agreement with the H1 measurement.

2.1 Conclusion

The H1 measurement of inclusive D^* cross sections in DIS in an increased phase space and using the full HERAII statistics has been presented. The data is well described by the FFNS calculations, but not by the ZM-VFNS calculation. The charm contribution to the proton structure function $F_2^{c\bar{c}}$ has been extracted. The extrapolation to the full phase space was performed with two predictions from HVQDIS and CASCADE. This D^* measurement is in good agreement with an independent H1 measurement using lifetime informations. $F_2^{c\bar{c}}$ is well described by all of the NLO calculations, so that one can conclude that the gluon PDF found in scaling violations of inclusive DIS cross section measurements agrees well with the gluon density in this measurement.

References

[1] F. D. Aaron *et al.* [H1 Collaboration], "Measurement of $D^{*\pm}$ Meson Production and Determination of F_2^{ccbar} at low Q2 in Deep-Inelastic Scattering at HERA," Eur. Phys. J. C **71** (2011) 1769 [arXiv:1106.1028 [hep-ex]].

[2] A. Aktas *et al.* [H1 Collaboration], Eur. Phys. J. **C51** (2007) 271 [hep-ex/0701023].

[3] A. Kwiatkowski, H. Spiesberger, and H.J. Mohring, HERACLES V4.6, Comp. Phys. Commun. **69** (1992) 155.

[4] H. Jung, RAPGAP V3.1, Comp. Phys. Commun. **86** (1995) 147.

[5] H. Jung, CASCADE V2.0, Comp. Phys. Commun. **143** (2002) 100.

[6] M. Bengtsson and T. Sjostrand, Z. Phys. **C37** (1988) 465.

[7] B.W. Harris and J. Smith, Nucl. Phys. **B452** (1995) 109 [hep-ph/9503484];
B.W. Harris and J. Smith, Phys. Rev. **D57** (1998) 2806 [hep-ph/9706334].

[8] G. Heinrich, B. A. Kniehl, Phys. Rev. **D70** (2004) 094035 [hep-ph/0409303];
C. Sandoval, Proc. of XVII International Workshop on Deep-Inelastic Scattering (DIS 2009), Madrid, 2009, arXiv:0908.0824;
C. Sandoval, "Inclusive Production of Hadrons in Neutral and Charged Current Deep Inelastic Scattering", Ph.D. Thesis, Univ. Hamburg (2009), DESY-THESIS-2009-044.

[9] F.D. Aaron *et al.* [H1 Collaboration], Eur. Phys. J. **C65** (2010) 89 [arXiv:0907.2643].

[10] F.D. Aaron *et al.* [H1 and ZEUS Collaboration], JHEP **1001** (2010) 109 [arXiv:0911.0884].

[11] H.L. Lai *et al.* [CTEQ Collaboration], Phys. Rev. **D82** (2010) 074024 [arXiv:1007.2241].

[12] A.D. Martin, W.J. Stirling, R.S. Thorne and G. Watt, Eur. Phys. J. **C63** (2009) 189 [arXiv:0901.0002].

[13] R.D. Ball *et al.*, Nucl. Phys. **B849** (2011) 296 [arXiv:1101.1300].

[14] S. Alekhin, J. Blümlein, S. Klein and S. Moch, Phys. Rev. **D81** (2010) 014032 [arXiv:0908.2766].